

# Patterned Nonadhesive Surfaces: Superhydrophobicity and Wetting Regime Transitions<sup>†</sup>

Michael Nosonovsky<sup>‡,||</sup> and Bharat Bhushan<sup>\*,§</sup>

National Institute of Standards and Technology, 100 Bureau Drive, Stop 8520, Gaithersburg, Maryland 20899-8520, and Nanotribology Laboratory for Information Storage and MEMS/NEMS(NLIM), The Ohio State University, 201 W. 19th Avenue, Columbus, Ohio 43210-1142

Received July 24, 2007. In Final Form: November 5, 2007

Nonadhesive and water-repellent surfaces are required for many tribological applications. We study mechanisms of wetting of patterned superhydrophobic Si surfaces, including the transition between various wetting regimes during microdroplet evaporation in environmental scanning electron microscopy (ESEM) and for contact angle and contact angle hysteresis measurements. Wetting involves interactions at different scale levels: macroscale (water droplet size), microscale (surface texture size), and nanoscale (molecular size). We propose a generalized formulation of the Wenzel and Cassie equations that is consistent with the broad range of experimental data. We show that the contact angle hysteresis involves two different mechanisms and how the transition from the metastable partially wetted (Cassie) state to the homogeneously wetted (Wenzel) state depends upon droplet size and surface pattern parameters.

## 1. Introduction

Numerous micro/nanotribological and micro/nanomechanical applications, such as the micro/nanoelectromechanical systems (MEMS/NEMS), require surfaces with low adhesion and stiction.<sup>1,2</sup> As the size of these devices decreases, the surface forces tend to dominate over the volume forces, and adhesion and stiction constitute a challenging problem that jeopardizes the proper operation of these devices. This makes the development of nonadhesive surfaces crucial for many of these emerging applications. It has been suggested that extremely water-repellent (superhydrophobic) surfaces produced by applying micropatterned roughness combined with hydrophobic coatings may satisfy the need for nonadhesive surfaces.<sup>3–8</sup>

Roughness-induced superhydrophobicity became an object of intensive study in recent years because of the emergence of superhydrophobic microtextured surfaces and their applicability in nanotechnology. Despite the apparent simplicity of the physical phenomena involved, there are a number of theoretical and practical problems related to the superhydrophobicity, which are still unsolved. Superhydrophobicity involves effects on the molecular, micrometer, and millimeter scales. On the macroscale, such a system as a water droplet upon a rough surface (Figure 1a) may be described with a simple set of equations governing the macroscale parameters (e.g., the contact angle). However, the state and behavior of the system may also depend upon the micro- and nanoscale parameters, and thus the macroscale parameters do not provide the closed set of variables for the

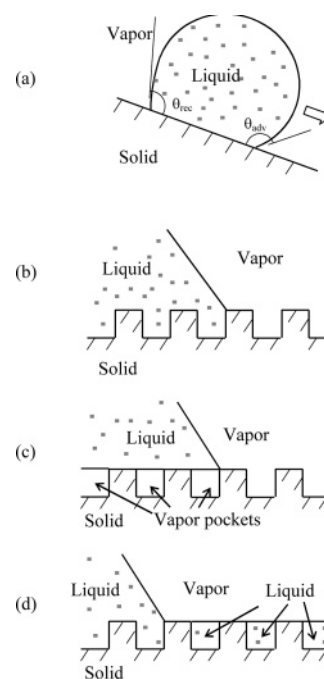


**Figure 1.** (a) Schematics of a droplet on a tilted substrate showing advancing ( $\theta_{adv}$ ) and receding ( $\theta_{rec}$ ) contact angles. The difference between these angles constitutes the contact angle hysteresis. Configurations are described by (b) the Wenzel equation for the homogeneous interface (eq 1), (c) the Cassie–Baxter equation for the composite interface with vapor (or air) pockets (eq 3), and (d) the Cassie equation for the homogeneous interface (eq 4).

description of the system, making the description in terms of the macroscale parameters incomplete. One particular question that is a subject of intensive argument is whether the wetting of superhydrophobic surfaces is a process that is determined by thermodynamic equations for the free surface energies or whether it is more adequately described by the kinetics of the triple line (the solid–liquid–vapor contact line). It has been shown experimentally that processes near or at the triple line determine the contact angle, whereas what happens under the droplet does not matter.<sup>9,10</sup> However, the so-called Wenzel and Cassie equations, which relate the contact angle of a liquid with a rough

<sup>†</sup> Part of the Molecular and Surface Forces special issue.

\* Corresponding author. E-mail: bhushan.2@osu.edu. Tel: 614-292-0651. Fax: 614-292-0325.

<sup>‡</sup> National Institute of Standards and Technology.

<sup>§</sup> The Ohio State University.

<sup>||</sup> Present address: Stevens Institute of Technology, Hoboken, NJ.

(1) Bhushan, B. *J. Vac. Sci. Technol., B* **2003**, *21*, 2262–2296

(2) Bhushan, B. *Springer Handbook of Nanotechnology*, 2nd ed.; Springer-Verlag: Heidelberg, Germany, 2007.

(3) Nosonovsky, M.; Bhushan, B. *Microsyst. Technol.* **2005**, *11*, 535–549.

(4) Nosonovsky, M.; Bhushan, B. *Microsyst. Technol.* **2006**, *12*, 231–237.

(5) Nosonovsky, M.; Bhushan, B. *Microsyst. Technol.* **2006**, *12*, 273–281.

(6) Nosonovsky M.; Bhushan B. *Microelectron. Eng.* **2007**, *84*, 382–386.

(7) Bhushan, B.; Nosonovsky M.; Jung, Y. C. *J. R. Soc. Interface* **2007**, *4*, 643–648

(8) Barbieri, L.; Wagner, E.; Hoffmann, P. *Langmuir* **2007**, *23*, 1723–1734.

or heterogeneous surface to that with a smooth homogeneous surface, are known to fit the experimental data well.<sup>7,8,11–13</sup> Therefore, the question remains as to under what circumstances the Wenzel and Cassie equations can be used.

Another problem is related to the coexistence of various wetting states, namely, the homogeneous (Wenzel) and composite (Cassie) states, their stability, and transitions between these states.<sup>14</sup> It is known from experiments that the transition from the Cassie to Wenzel state is irreversible.<sup>7,8,14</sup> Whereas such a transition can be induced, for example, by applying pressure or force to the droplet,<sup>8</sup> an electric voltage,<sup>15–16</sup> light for photocatalytic texture,<sup>17</sup> and vibration,<sup>18</sup> the opposite transition has never been observed, although there is no apparent reason for that. Several approaches have been proposed to explain the Cassie–Wenzel transition, including the approach based on the net surface energy levels of the two states,<sup>14</sup> the balance between the droplet weight and surface tension force,<sup>19</sup> the history of the system,<sup>20</sup> the droplet curvature,<sup>21</sup> the dynamic destabilizing effects and gradual stochastic transition,<sup>4</sup> and the multiscale roughness.<sup>11</sup> There is experimental evidence in support of every one of these approaches; however, there is still no convincing explanation of the mechanism of transition, and as in the case of the Wenzel and Cassie equations, it is not clear whether the transition is governed by interactions at the triple line or at the interface under the droplet.

In this article, we will consider the range of applicability of the Wenzel and Cassie equations in light of the available experimental data and theoretical considerations. We propose a generalized form of these equations that explains the available experimental data and show that the triple line and interface interactions determine the contact angle. Environmental scanning electron microscopy (ESEM) provides the way to observe in situ condensation and evaporation on the micro and nanoscale.<sup>22,23</sup> We study the Cassie–Wenzel transition using the ESEM observations of microdroplet evaporation upon micropatterned structures. We will show that the droplet radius at the transition scales well with the geometrical dimensions of the micropattern. This provides new evidence on wetting as a process governed by interactions on different size scales, from the macroscale down to the nanoscale.

## 2. Generalized Wenzel–Cassie Equations

The Wenzel<sup>24</sup> equation, which was derived for the homogeneous interface (Figure 1b) using the surface force balance and empirical considerations, relates the contact angle of a water droplet upon a rough solid surface,  $\theta$ , with that upon a smooth surface,  $\theta_0$ , through the nondimensional surface roughness factor,

$R_f \geq 1$ , which is equal to the ratio of the surface area to its flat projection

$$\cos \theta = R_f \cos \theta_0 \quad (1)$$

In a similar manner, for a surface composed of two fractions (one with fractional area  $f_1$  and contact angle  $\theta_1$  and the other with  $f_2$  and  $\theta_2$  ( $f_1 + f_2 = 1$ )), the contact angle is given by the Cassie equation

$$\cos \theta = f_1 \cos \theta_1 + f_2 \cos \theta_2 \quad (2)$$

For the case of a composite interface (Figure 1c) consisting of the solid–liquid fraction ( $f_1 = f_{SL}$ ,  $\theta_1 = \theta_0$ ) and the liquid–vapor fraction ( $f_2 = 1 - f_{SL}$ ,  $\cos \theta_2 = -1$ ), combining eqs 1 and 2 yields the Cassie–Baxter equation<sup>25</sup>

$$\cos \theta = f_{SL} R_f \cos \theta_0 - 1 + f_{SL} \quad (3)$$

The opposite limiting case of  $\cos \theta_2 = 1$  (where  $\theta_2 = 0^\circ$  corresponds to water-on-water contact) yields

$$\cos \theta = 1 + f_{SL} (\cos \theta_0 - 1) \quad (4)$$

Equation 4 is sometimes used<sup>26</sup> for the homogeneous interface instead of eq 1 if the rough surface is covered by holes filled with water (Figure 1d).

The Cassie equation (eq 2) is based on the assumption that the heterogeneous surface is composed of well-separated distinct patches of different materials so that the free surface energy can be averaged. It has also been argued that when the size of the chemical heterogeneities is very small (of atomic or molecular dimensions) the quantity that should be averaged is not the energy but the dipole moment of a macromolecule,<sup>27</sup> and eq 2 may be replaced by

$$(1 + \cos \theta)^2 = f_1 (1 + \cos \theta_1)^2 + f_2 (1 + \cos \theta_2)^2 \quad (5)$$

Experimental studies of polymers with different functional groups show good agreement with eq 5.<sup>28</sup>

Later investigations put the Wenzel and Cassie equations into a thermodynamic framework; however, they also showed that there is no unique value of the contact angle for a rough or heterogeneous surface.<sup>29–31</sup> The contact angle can be in a range of values between the so-called receding contact angle,  $\theta_{\text{rec}}$ , and the advancing contact angle,  $\theta_{\text{adv}}$ . The system tends to achieve the receding contact angle when liquid is removed (for example, at the rear end of a moving droplet), whereas the advancing contact angle is achieved when liquid is added (for example, at the front end of a moving droplet). When no liquid is added or removed, the system tends to have a static or “most stable” contact angle, which can be approximated by eqs 1–3. The difference between  $\theta_{\text{adv}}$  and  $\theta_{\text{rec}}$  is known as contact angle hysteresis and reflects the fundamental asymmetry of wetting and dewetting and the irreversibility of the wetting/dewetting cycle. Although

- (9) Extrand, C. W. *Langmuir* **2003**, *19*, 3793–3796.  
 (10) Gao, L.; McCarthy, T. J. *Langmuir* **2007**, *23*, 3762–3765.  
 (11) Nosonovsky, M. *Langmuir* **2007**, *23*, 3157–3161.  
 (12) Nosonovsky, M. *J. Chem. Phys.* **2007**, *126*, 224701.  
 (13) Nosonovsky, M. *Langmuir* **2007**, *23*, 9919–9920.  
 (14) Lafuma, A.; Quéré, D. *Nat. Mater.* **2003**, *2*, 457–460.  
 (15) Krupenkin, T. N.; Taylor, J. A.; Schneider, T. M.; Yang, S. *Langmuir* **2004**, *20*, 3824–3827.  
 (16) Bahadur, V.; Garimella, S. V. *Langmuir* **2007**, *23*, 4918–4924.  
 (17) Feng, X. J.; Feng, L.; Jin, M. H.; Zhai, J.; Jiang, L.; Zhu, D. B. *J. Am. Chem. Soc.* **2004**, *126*, 62–63.  
 (18) Bormashenko, E.; Pogreb, R.; Whyman, G.; Erlich, M. *Langmuir* **2007**, *23*, 6501–6503.  
 (19) Extrand, C. W. *Langmuir* **2002**, *18*, 7991–7999.  
 (20) Patankar, N. A. *Langmuir* **2004**, *20*, 7097–7102.  
 (21) Quéré, D. *Rep. Prog. Phys.* **2005**, *68*, 2495–2535.  
 (22) Cheng Y.; Rodak D. E.; Angelopoulos A.; Gacek T. *Appl. Phys. Lett.* **2005**, *87*, 194112–194112–3.  
 (23) Bormashenko, E.; Bormashenko, Y.; Stein, T.; Whyman, G.; Pogreb, R.; Barkay, Z. *Langmuir* **2007**, *23*, 4378–4382.  
 (24) Wenzel, R. N. *Ind. Eng. Chem.* **1936**, *28*, 988–994.

- (25) Cassie, A.; Baxter, S. *Trans. Faraday Soc.* **1944**, *40*, 546–551.  
 (26) de Gennes, P. G.; Brochard-Wyart, F.; Quéré, D. *Capillarity and Wetting Phenomena*; Springer: Berlin, 2003.  
 (27) Israelachvili, J. N.; Gee, M. L. *Langmuir* **1989**, *5*, 288–289.  
 (28) Tretinnikov, O. N. Wettability and Microstructure of Polymer Surfaces: Stereochemical and Conformational Aspects. In *Apparent and Microscopic Contact Angles*; Drelich, J., Laskowski, J. S., Mittal, K. L., Eds.: VSP: Utrecht, The Netherlands, 2000; pp 111–128.  
 (29) Johnson, R. E.; Dettre, R. H. Contact Angle Hysteresis. In *Contact Angle, Wettability, and Adhesion*; Fowke, F. M., Ed.; Advances in Chemistry Series; American Chemical Society: Washington, DC, 1964; Vol. 43, pp 112–135.  
 (30) Marmur, A. *Langmuir* **2003**, *19*, 8343–8348.  
 (31) Li, W.; Amirfazli, A. *J. Colloid. Interface Sci.* **2006**, *292*, 195–201.

for surfaces with roughness carefully controlled on the molecular scale it is possible to achieve contact angle hysteresis as low as  $<1^\circ$ ,<sup>32</sup> it cannot be eliminated completely because even atomically smooth surfaces have a certain roughness and heterogeneity. Contact angle hysteresis is a measure of energy dissipation during the flow of a droplet along a solid surface. A water-repellent surface should have low contact angle hysteresis to allow water to flow easily along the surface.

It is emphasized that the contact angle provided by eqs 1–5 is a macroscale parameter, so it is sometimes called the apparent contact angle. The actual angles under which the liquid–vapor interface comes into contact with the solid surface on the micro- and nanoscale can be different. There are several reasons for this. First, water molecules tend to form a thin layer upon the surfaces of many materials. This is because of a long-distance van der Waals adhesion force that results in the so-called disjoining pressure.<sup>33</sup> This pressure is dependent upon the liquid layer thickness and may lead to the formation of stable thin films. In this case, the shape of the droplet near the triple line transforms gradually from the spherical surface into a precursor layer, and thus the nanoscale contact angle is much smaller than the apparent contact angle. In addition, adsorbed water monolayers and multilayers are common for many materials. Second, even carefully prepared atomically smooth surfaces exhibit a certain roughness and chemical heterogeneity. At first, water tends to cover the hydrophilic spots with high surface energy and low contact angle.<sup>34</sup> The tilt angle due to the roughness can also contribute to the apparent contact angle. Third, the very concept of the static contact angle is not well-defined. For practical purposes, the contact angle, which is formed after a droplet is gently placed upon a surface and stops propagating, is considered to be the static contact angle. However, depositing the droplet involves adding liquid whereas leaving it may involve evaporation, so it is difficult to avoid dynamic effects. Fourth, for small droplets and curved triple lines, the effect of the contact line tension may be significant. Molecules at the surface of a liquid or solid phase have higher energy because they are bonded to fewer molecules than are those in the bulk. This leads to surface tension and surface energy. In a similar manner, molecules at the edge have fewer bonds than those at the surface, which leads to the line tension and the curvature dependence of the surface energy. This effect becomes important when the radius of curvature of the droplet is comparable with the so-called Tolman length, normally on the order of the molecular size.<sup>35</sup> Although the size of the droplet is usually much larger than the Tolman length, the triple line on the nanoscale can be curved, so the line tension effects become important.<sup>36</sup> Thus, whereas the contact angle is a convenient macroscale parameter, wetting is governed by interactions on the micro- and nanoscale, which determine the contact angle hysteresis and other wetting properties.

Micropatterned surfaces are the main object of interest because of their potential for applications. For a micropatterned surface built from flat-topped columns ( $R_f = 1$ ), the contact angle hysteresis involves a term that is inherent in the nominally smooth surface and a term that is dependent upon the surface roughness,  $H_r$ ,

(32) Gupta, P.; Ulman, A.; Fanfan, F.; Korniaikov, A.; Loos, K. *J. Am. Chem. Soc.* **2005**, *127*, 4–5.

(33) Derjaguin, B. V.; Churaev, N. V. *J. Colloid. Interface Sci.* **1974**, *49*, 249–255.

(34) Checco, A.; Guenoun, P.; Daillant, J. *Phys. Rev. Lett.* **2003**, *91*, 186101.

(35) Anisimov, M. A. *Phys. Rev. Lett.* **2007**, *98*, 035702.

(36) Pompe, T.; Fery, A.; Herminghaus, S. Measurement of Contact Line Tension by Analysis of the Three-Phase Boundary with Nanometer Resolution. In *Apparent and Microscopic Contact Angles*; Drelich, J., Laskowski, J. S., Mittal, K. L., Eds.; VSP: Utrecht, The Netherlands, 2000; pp 3–12.

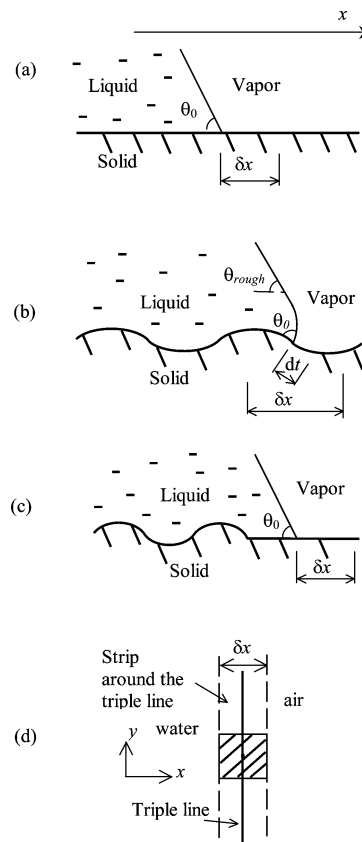


**Figure 2.** Liquid front in contact with (a) a smooth solid surface and (b) a rough solid surface. (c) Surface roughness under the bulk of the droplet does not affect the contact angle.<sup>13</sup> (d) Averaged value of roughness/heterogeneity parameters at the triple line is obtained by integration along the square area (dashed) with the side  $\delta x$ .

$$\cos \theta_{adv} - \cos \theta_{rec} = f_{SL}(\cos \theta_{adv0} - \cos \theta_{rec0}) + H_r \quad (6)$$

where  $\theta_{adv0}$  and  $\theta_{rec0}$  are the advancing and receding contact angles for the smooth surface.<sup>7,12</sup> The first term on the right-hand side of eq 6, which corresponds to the inherent contact angle hysteresis of a smooth surface, is proportional to the fraction of the solid–liquid contact area,  $f_{SL}$ . The second term,  $H_r$ , may be assumed to be proportional to the length density of the pillar edges or, in other words, to the length density of the triple line.<sup>7</sup> Thus, eq 6 involves both the term proportional to the solid–liquid interface area and the term proportional to the triple-line length.

Gao and McCarthy<sup>10</sup> showed experimentally that the contact angle of a droplet is defined by the triple line and does not depend upon the roughness under the bulk of the droplet. A similar result for chemically heterogeneous surfaces was obtained by Extrand.<sup>9</sup> Gao and McCarthy concluded that the Wenzel and Cassie equations “should be used with the knowledge of their fault”.<sup>10</sup> The question remained, however, as to under what circumstances the Wenzel and Cassie equations can be safely used and under what circumstances they become irrelevant. In their paper, entitled “How Wenzel and Cassie Were Wrong”, Gao and McCarthy<sup>10</sup> did not provide any suggestion as to when these equations can be used, but their paper initiated a discussion. Nosonovsky<sup>13</sup> suggested a generalization of these equations for the case of nonuniform roughness. Independently and simultaneously, a similar generalization for the axisymmetric case was proposed by McHale.<sup>37</sup>

(37) McHale, G. *Langmuir* **2007**, *23*, 8200–8205.

**Table 1. Wetting of a Superhydrophobic Surface as a Multiscale Process**

scale level	characteristic length	parameters	phenomena	interface
macroscale	droplet radius (mm)	contact angle, droplet radius	contact angle hysteresis	2D
microscale	roughness detail ( $\mu\text{m}$ )	shape of the droplet, position of the liquid–vapor interface ( $h$ )	kinetic effects	3D solid surface, 2D liquid surface
nanoscale	molecular heterogeneity (nm)	molecular description	thermodynamic and dynamic effects	3D

The most convenient way to handle the Wenzel and Cassie equations is to use the principle of virtual work and consider a liquid to advance over a small distance  $\delta x$ . For a liquid front propagating along a rough 2D profile (Figure 2a,b), the derivative of the surface free energy (per liquid front length)  $W$  with respect to the profile length  $l$  yields the surface tension force  $\sigma = dW/dl = \gamma_{SL} - \gamma_{SV}$ . The quantity of practical interest is the component of the tension force that corresponds to the advancing of the liquid front in the horizontal direction for  $dx$ . This component is given by  $dW/dx = (dW/dl)(dl/dx) = (\gamma_{SL} - \gamma_{SV}) dl/dx$ . The local value of  $dW/dx$  depends upon  $x$ ; however, if the virtual distance  $\delta x$  is large enough, then the average value of  $dW/dx$  can be considered (where the bar means the average value over the distance  $\delta x$ ). It is noted that the derivative  $R_f = dl/dx$  is equal to the Wenzel roughness factor. Therefore, the Young equation, which relates the contact angle to the solid, liquid, and vapor interface tensions,  $\gamma_{LV} \cos \theta = \gamma_{SV} - \gamma_{SL}$ , is modified as<sup>13</sup>

$$\gamma_{LV} \cos \theta = R_f(\gamma_{SV} - \gamma_{SL}) \quad (7)$$

The empirical Wenzel equation (eq 1) is a consequence of eq 7 combined with the Young equation.

Nosonovsky<sup>13</sup> suggested that for a more complicated case of a nonuniform roughness, given by the profile  $z(x)$ , the local value of  $r(x) = dl/dx = (1+(dz/dx)^2)^{1/2}$  matters. In the cases that were studied experimentally by Gao and McCarthy<sup>10</sup> and Extrand,<sup>9</sup> the roughness was present ( $r > 1$ ) under the bulk of the droplet but there was no roughness ( $r = 0$ ) at the triple line, and the contact angle was given by eq 1 (Figure 2c). In the general case of a 3D rough surface  $z(x, y)$ , the roughness factor can be defined as a function of the coordinates  $r(x, y) = (1+(dz/dx)^2+(dz/dy)^2)^{1/2}$ .

Whereas eq 1 is valid for uniformly rough surfaces, that is, for surfaces with  $r = \text{const}$ , for nonuniformly rough surfaces the generalized Wenzel equation is formulated to determine the local

contact angle (a function of  $x$  and  $y$ ) with a rough surfaces at the triple line<sup>13,37</sup>

$$\cos \theta = r(x, y)\cos \theta_0 \quad (8)$$

Equation 8 is consistent with the experimental results of the scholars, who showed that roughness beneath the droplet does not affect the contact angle because it predicts that only roughness at the triple line matters. It is also consistent with the results of the researchers who confirmed the Wenzel equation (for the case of uniform roughness) and of those who reported that only the triple line matters (for nonuniform roughness) (Table 2).

The Cassie equation for the composite surface can be generalized in a similar manner by introducing the spatial dependence of the local densities,  $f_1$  and  $f_2$  of the solid–liquid interface with the contact angle, as a function of  $x$  and  $y$ , given by

$$\cos \theta_{\text{composite}} = f_1(x, y)\cos \theta_1 + f_2(x, y)\cos \theta_2 \quad (9)$$

where  $f_1 + f_2 = 1$  and  $\theta_1$  and  $\theta_2$  are contact angles of the two components.<sup>13,37</sup>

Equations 8 and 9 are useful only if the average values of  $r$ ,  $f_1$ , and  $f_2$  are constant at the triple line, thus providing a unique value of the apparent contact angle. An example of such situation is the 2D configuration, which was discussed above. Another example is when the roughness/heterogeneity has an axisymmetric distribution with the droplets sitting at the center, as was considered by McHale.<sup>37</sup> The main difference between the conventional Wenzel and Cassie–Baxter models and the proposed model is that in the conventional approach the averaging was performed over the entire area whereas in our approach the averaging was performed locally in the vicinity of the triple line.

The important question remains as to over what area the averaging should be performed in order to obtain  $r$ ,  $f_1$ , and  $f_2$ . The triple line is an idealized 1D object with no width; however, the averaging is performed over a certain area. It is clear from the above analysis that in the case of a rough surface the value of the roughness factor at a given point of the triple line is obtained by averaging over the area with the characteristic size  $\delta x$  such that  $\delta x$  is greater than the size of the roughness details (Figure 2d). The same consideration also applies to  $f_1$  and  $f_2$  of a heterogeneous surface. In the past, some scholars have suggested that roughness/heterogeneity details should be comparable to the thickness of the liquid–vapor interface and thus “the roughness would have to be of molecular dimensions to alter the equilibrium conditions”,<sup>38</sup> whereas others have claimed that roughness/heterogeneity details should be small compared with the linear

**Table 2. Summary of Experimental Results for Uniform<sup>9,10</sup> and Nonuniform<sup>7,8</sup> Rough and Chemically Heterogeneous Surfaces<sup>a</sup>**

experiment	roughness/hydrophobicity at the triple line and at the rest of the surface	roughness at the bulk (under the droplet)	experimental contact angle (compared with that at the rest of the surface)	theoretical contact angle, Wenzel and Cassie equations (eqs 1 and 3)	theoretical contact angle, generalized Wenzel and Cassie equations (eqs 8 and 9)
Gao and McCarthy <sup>10</sup>	hydrophobic	hydrophilic	not changed	decreased	not changed
Extrand <sup>9</sup>	rough	smooth	not changed	decreased	not changed
	smooth	rough	not changed	increased	not changed
Bhushan et al. <sup>7</sup> Barbieri et al. <sup>8</sup>	hydrophilic	hydrophobic	not changed	increased	not changed
	hydrophobic	hydrophilic	not changed	decreased	not changed
	rough	rough	increased	increased	increased
	rough	rough	increased	increased	increased

<sup>a</sup> For nonuniform surfaces, the results shown are for droplets that are larger than the islands of nonuniformity. Detailed quantitative values of the contact angle in various sets of experiments can be found in the referenced sources.<sup>7–10</sup>

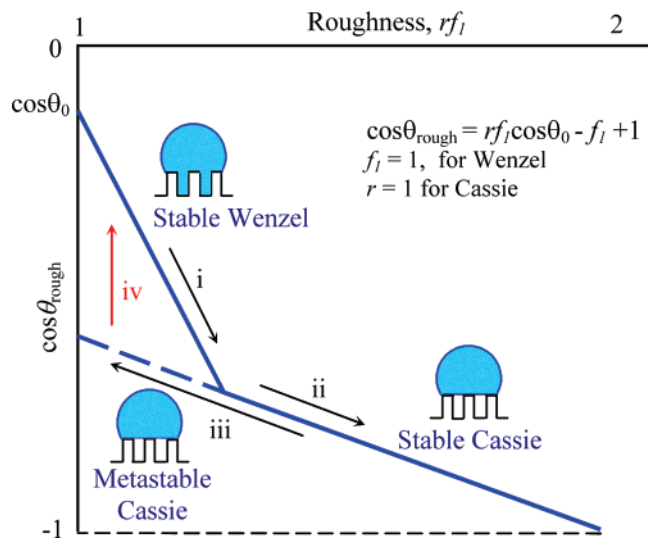


**Figure 3.** Wetting hysteresis for a superhydrophobic surface. Contact angle as a function of roughness. The intersection of the Wenzel and Cassie regime lines corresponds to equal Wenzel and Cassie state free energies, whereas the transition shown by the arrow (iv) corresponds to significant energy dissipation, thus it is irreversible.

size of the droplet.<sup>7,8,29–31</sup> When the liquid–vapor interface is studied on the length scale of roughness/heterogeneity details, the local contact angle,  $\theta_0$ , is given by eq 1. The liquid–vapor interface on that scale has perturbations caused by the roughness/heterogeneity, and the scale of the perturbations is the same as the scale of the roughness/heterogeneity details. However, when the same interface is studied on a larger scale, the effect of the perturbation vanishes, and the apparent contact angle is given by eqs 8 and 9. A similar conclusion can be drawn from the simulation results obtained by Kusumaatmaja and Yeomans,<sup>39</sup> who showed that contact angle hysteresis is sensitive to the details of the surface patterning.

### 3. Cassie–Wenzel Transition and Contact Angle Hysteresis

It is known from experimental observations that the transition from the Cassie to the Wenzel state is an irreversible event.<sup>7,8,14</sup> Whereas such a transition can be induced, for example, by applying pressure to the droplet, the opposite transition has never been observed, although there is no apparent reason for that. Several approaches have been proposed for investigation of the Cassie–Wenzel transition. Lafuma and Quéré<sup>14</sup> suggested that the transition takes place when the net surface energy of the Wenzel state becomes equal to that of the Cassie state or, in other words, when the contact angle predicted by the Cassie equation is equal to that predicted by the Wenzel equation. They noticed that in a certain case the transition does not occur even when it is energetically profitable and considered such a Cassie state to be metastable. Extrand<sup>19</sup> suggested that the weight of the droplet is responsible for the transition and proposed the contact line density model, according to which the transition takes place when the weight exceeds the surface tension force at the triple line. Patankar<sup>20</sup> suggested that which of the two states is realized may depend upon how the droplet was formed, that is, upon the history of the system. Quéré<sup>21</sup> also suggested that the droplet curvature (which depends upon the pressure difference between the inside and outside of the droplet) governs the transition. Nosonovsky and Bhushan<sup>3</sup> suggested that the transition is a

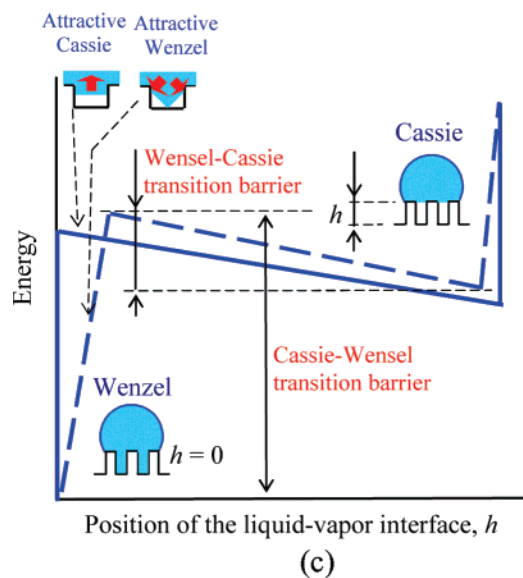
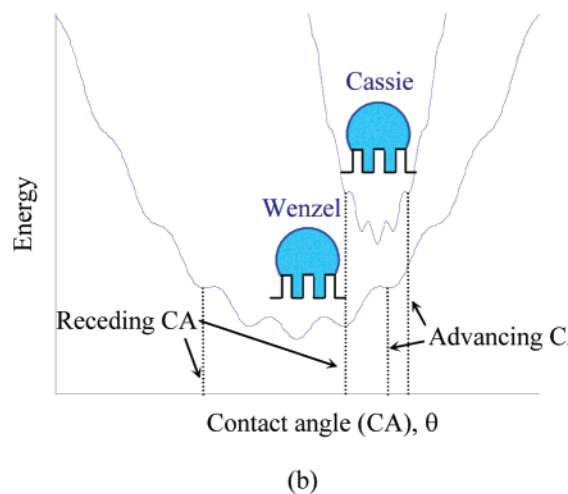
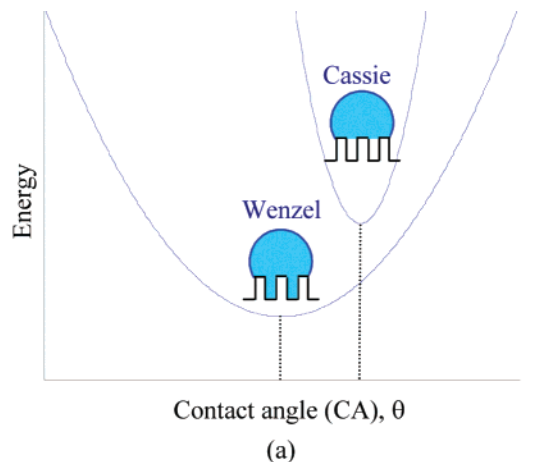


**Figure 4.** Schematics of net free-energy profiles. (a) Macroscale description; energy minima correspond to the Wenzel and Cassie states. (b) Microscale description with multiple energy minima due to surface texture. The largest and smallest values of the energy minimum correspond to the advancing and receding contact angles. (c) Origin of the two branches (Wenzel and Cassie) is found when a dependence of energy upon  $h$  is considered for the microscale description (solid line) and nanoscale imperfections (dashed line) based on ref 4. When the nanoscale imperfection is introduced, it is observed that the Wenzel state corresponds to an energy minimum and the energy barrier for the Wenzel–Cassie transition is much smaller than for the opposite transition.

(38) Bartell, F. E.; Shepard, J. W. *J. Phys. Chem.* **1953**, *57*, 455–458.  
 (39) Kusumaatmaja, H.; Yeomans, J. M. *Langmuir* **2007**, *23*, 6019–6032.

dynamic process of destabilization and identified possible destabilizing factors. They also considered mechanisms on various scale levels that lead to this transition.<sup>40</sup> It has been also suggested that the curvature of multiscale roughness defines the stability of the Cassie state<sup>6,11</sup> and that the transition is a stochastic gradual process.<sup>6,18,41</sup> Numerous experimental results support many of these approaches; however, it is not clear which particular mechanism prevails.

There is an asymmetry between the wetting and dewetting processes because droplet nucleation requires less energy than vapor bubble nucleation (cavitation). During wetting, which involves the creation of the solid–liquid interface, less energy is released than the amount required for dewetting or destroying the solid–liquid interface as a result of so-called adhesion hysteresis.<sup>42</sup> Adhesion hysteresis is one of the reasons that leads to contact angle hysteresis, and it also results in hysteresis of the Wenzel–Cassie state transition. Figure 3 shows the contact angle of a rough surface as a function of surface roughness (which is measured, for the Wenzel regime, by  $r > 1$ ,  $f_1 = 1$  and for the Cassie regime by  $f_1 < 1$ ,  $r = 1$ ). It is noted that at a certain point, given by  $r = f_1 - (1 - f_1)/\cos \theta_1$ , the lines corresponding to the Wenzel and Cassie regimes intersect. This point corresponds to an equal net energy of the Cassie and Wenzel states. For a lower roughness (e.g., larger pitch between the pillars), the Wenzel state is more energetically profitable, whereas for a higher roughness the Cassie state is more energetically profitable.

Figure 3 also shows that an increase in roughness may lead to the transition between the Wenzel and Cassie regimes at the intersection point. With decreasing roughness, the system is expected to transition to the Wenzel state. However, experiments show<sup>7</sup> that, despite the energy of the Wenzel state being lower than that of the Cassie state, the transition does not necessarily occur and the droplet may remain in the metastable Cassie state. This is because there are energy barriers associated with the transition, which occurs because of destabilization by dynamic effects (such as waves and vibration).

To understand the contact angle hysteresis and transition between the Cassie and Wenzel states, the shape of the free surface energy profile can be analyzed. The free surface energy of a droplet upon a smooth surface as a function of the contact angle has a distinct minimum, which corresponds to the most stable contact angle.<sup>29</sup> As shown in Figure 4a, the macroscale profile of the net surface energy allows us to find the contact angle (corresponding to energy minimums); however, it fails to predict the contact angle hysteresis and Cassie–Wenzel transition, which are governed by micro- and nanoscale effects. As soon as the microscale substrate roughness is introduced, the droplet shape can no longer be considered to be an ideal truncated sphere, and energy profiles have multiple-energy minimums corresponding to the location of the pillars (Figure 4b). The microscale energy profile (solid line) has numerous energy maxima and minima due to the surface micropattern. Whereas the exact calculation of the energy profile for a 3D droplet is complicated, a qualitative shape may be obtained by assuming a periodic sinusoidal dependence<sup>29</sup> superimposed upon the macroscale profile, as shown in Figure 4b. Thus, the advancing and receding contact angles can be identified as the maximum and the minimum possible contact angles corresponding to energy-minimum points. However, the transition between the Wenzel and Cassie branches still cannot be explained. Note also that Figure 4b qualitatively

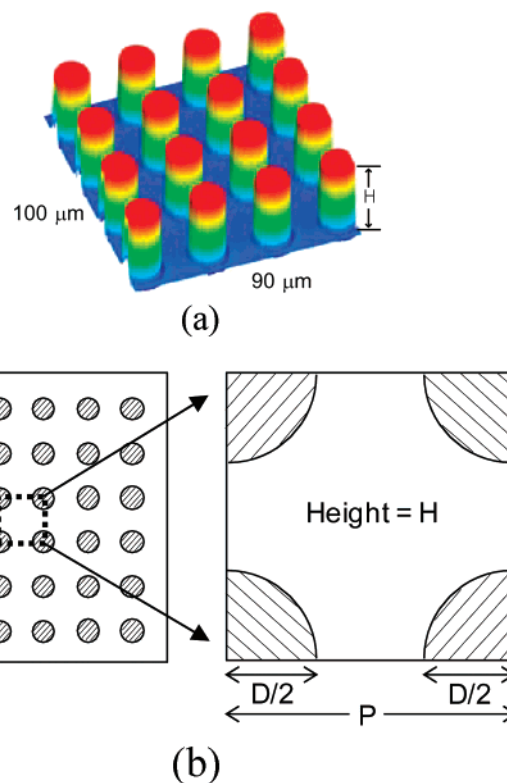


**Figure 5.** (a) Optical profiler image and (b) schematic of the patterned surface.

explains the hysteresis due to the kinetic effect of the pillars but not the inherited adhesion hysteresis, which is characterized by the molecular-scale length and cannot be captured by the microscale model.

The energy profile as a function of the contact angle does not provide any information on how the transition between the Cassie and Wenzel states occurs because two states correspond to completely isolated branches of the energy profile in Figure 4a,b. However, the energy may depend not only upon the contact angle but also upon micro/nanoscale parameters such as the vertical position of the liquid–vapor interface under the droplet,  $h$  (assuming that the interface is a horizontal plane), or similar geometrical parameters (assuming a more complicated shape of the interface). To investigate the Wenzel–Cassie transition, the dependence of the energy upon these parameters should be studied. We assume that the liquid–vapor interface under the droplet is a flat horizontal plane. When such vapor-layer thickness or the vertical position of the liquid–vapor interface,  $h$ , is introduced, the energy can be studied as a function of the droplet shape, the contact angle, and  $h$  (Figure 4c). For an ideal situation, the energy profile has an abrupt minimum at the point corresponding to the Wenzel state, which corresponds to the sudden net energy change per interface area due to destroying solid–vapor and liquid–vapor interfaces,  $\gamma_{SL} - \gamma_{SV} - \gamma_{LV} = -\gamma_{LV}(\cos \theta + 1)$  (Figure 4c). Thus, the energy (per unit length) decreases linearly as  $E = -\gamma_{LV}(\cos \theta + 1)h$  from the Wenzel to Cassie state, and no energy minimum is found.

In a more realistic case, the liquid–vapor interface cannot be considered horizontal because of nanoscale imperfectness or dynamic effects such as capillary waves.<sup>4</sup> The typical size of the imperfections is much smaller than the size of details of the surface texture and thus is on the molecular scale. The height of the interface,  $h$ , can now be treated as an average height. For example, the inclined (triangular) shape is shown in Figure 4c, with the interface coming under the angle  $\alpha = 45^\circ$  to the pillar,

(40) Nosonovsky, M.; Bhushan, B. *Nano Lett.* **2007**, *7*, 2633–2637.

(41) Ishino, C.; Okumura, K. *Europhys. Lett.* **2006**, *76*, 464–470.

(42) Ruths, M.; Israelachvili, J. N. *Surface Forces and Nanorheology of Molecularly Thin Films*; In *Springer Handbook of Nanotechnology*, 2nd ed.; Bhushan, B., Ed.; Springer-Verlag: Berlin, 2007; pp 859–924.

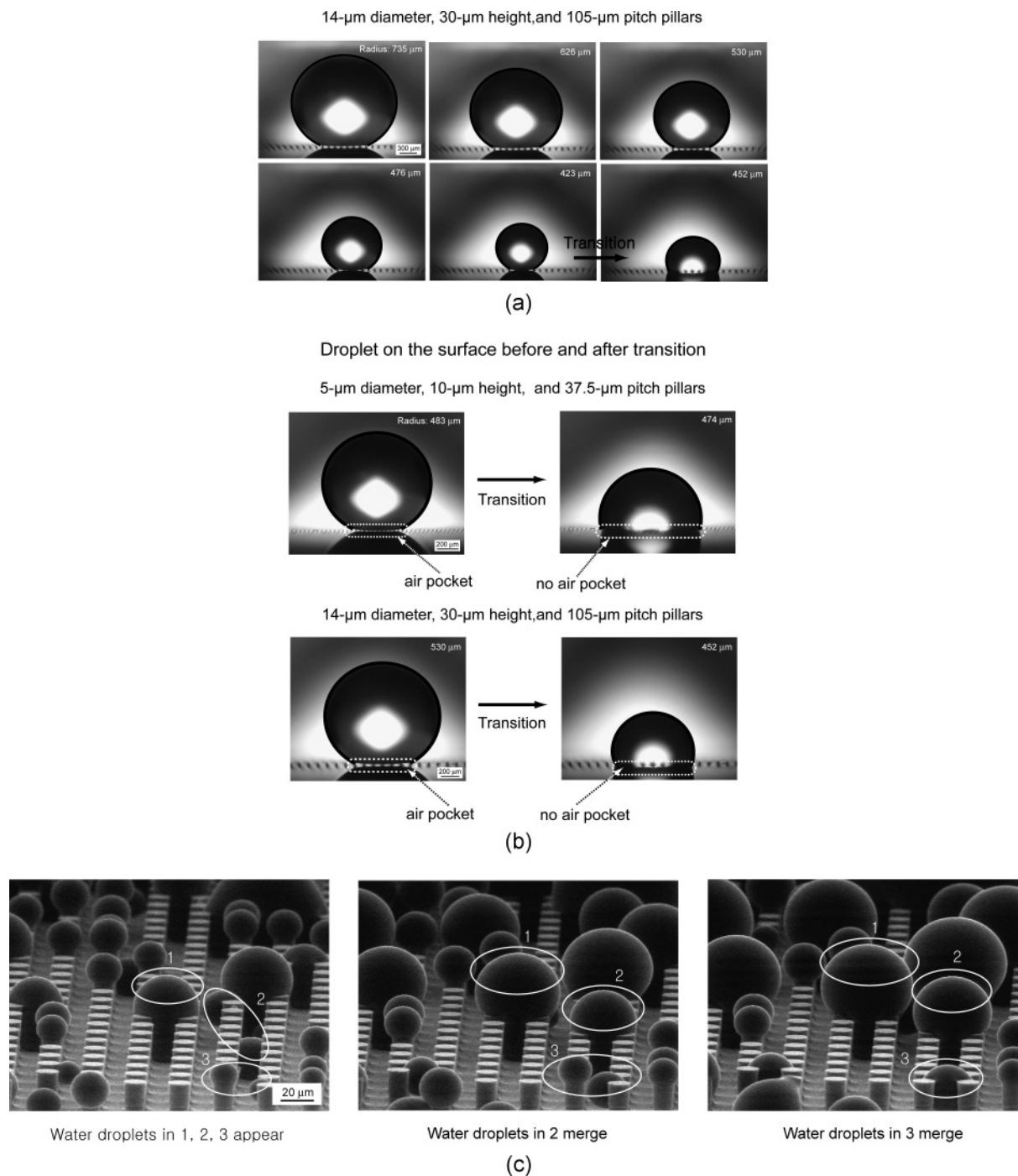


**Figure 6.** Microdroplets upon the patterned surface: (a) Cassie–Wenzel transition during evaporation. (b) ESEM micrographs of growing and merging droplets during condensation. No transition from the Wenzel to Cassie regime takes place. The Cassie–Wenzel transition is irreversible as a result of the asymmetry of wetting and dewetting.<sup>43</sup>

and the energy change is given by  $E = \gamma_{LV}(\cos \alpha - \cos \theta)h$ . The energy profile may have a piecewise shape,<sup>4</sup> as shown by the dashed line. In this case, the Wenzel state becomes the second attractor for the system. It is seen that there are two equilibria that correspond to the Wenzel and Cassie states, with the Wenzel state corresponding to a much lower energy level. The energy dependence upon  $h$  governs the transition between the two states, and it is observed that a much larger energy barrier exists for the transition from the Wenzel to Cassie state than for the opposite transition. This is why the first transition has never been observed experimentally.

To summarize, we showed that the contact angle hysteresis and Cassie–Wenzel transition cannot be determined from the

macroscale equations but are governed by micro- and nanoscale phenomena. Our theoretical arguments are supported by our experimental data on micropatterned surfaces.

#### 4. ESEM Study of the Cassie–Wenzel Transition

We studied two series of patterned Si surfaces, covered with a monolayer of hydrophobic tetrahydroperfluorodecyltrichlorosilane (contact angle with a nominally flat surface,  $\theta_0 = 109^\circ$ ; advancing and receding contact angle are  $\theta_{adv0} = 116^\circ$  and  $\theta_{rec0} = 82^\circ$ ), formed by flat-topped cylindrical pillars. Series 1 had pillars with diameter  $D = 5 \mu\text{m}$ , height  $H = 10 \mu\text{m}$ , and pitch values  $P = 7, 7.5, 10, 12.5, 25, 37.5, 45, 60, \text{ and } 75 \mu\text{m}$ , whereas series 2 had  $D = 14 \mu\text{m}$ ,  $H = 30 \mu\text{m}$ , and  $P = 21, 23, 26, 35,$

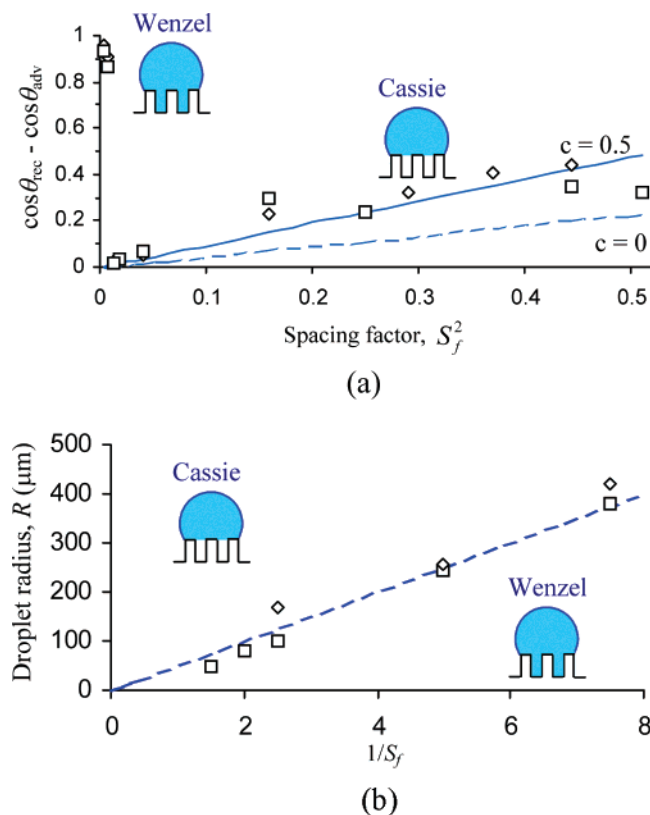


**Figure 7.** (a) Contact angle hysteresis as a function of  $S_f$  for the first ( $\square$ ) and second ( $\diamond$ ) series of experiments compared with the theoretically predicted values of  $\cos \theta_{\text{adv}} - \cos \theta_{\text{rec}} = (D/P)^2(\pi/4)(\cos \theta_{\text{adv}0} - \cos \theta_{\text{rec}0}) + c(D/P)^2$ , where  $c$  is a proportionality constant. It is observed that when only the adhesion hysteresis/interface energy term is considered ( $c = 0$ ) the theoretical values are underestimated by about half, whereas  $c = 0.5$  provides a good fit. Therefore, the contribution of adhesion hysteresis is of the same order of magnitude as the contribution kinetic effects. (b) Droplet radius,  $R$ , for the Cassie–Wenzel transition as a function of  $P/D = 1/S_f$ . It is observed that the transition takes place at a constant value of  $RD/P \approx 50 \mu\text{m}$  (---). This shows that the transition is a linear phenomenon.

70, 105, 126, 168, and 210  $\mu\text{m}$  (Figure 5). It is convenient to introduce the spacing factor  $S_f = D/P$ .<sup>6,7</sup> The contact angle and contact angle hysteresis of millimeter-sized water droplets on the samples were measured. In addition, the contact angle and the Wenzel–Cassie transition during the evaporation/condensation of microscale droplets in the ESEM were studied (Figure 6).<sup>43</sup> The transition from Cassie to Wenzel regimes was observed during droplet evaporation. It might be expected that the opposite transition could occur during the opposite process of droplet condensation; however, such an opposite transition does not occur.

We found that the contact angle hysteresis involves two terms: the term  $S_f^2(\pi/4)(\cos \theta_{\text{adv}0} - \cos \theta_{\text{rec}0})$  corresponding to adhesion hysteresis (which is found even at a nominally flat surface and is a result of molecular-scale imperfectness) and the term  $H_f \propto D/P^2$  corresponding to microscale roughness and proportional to the edge line density. Thus, the contact angle hysteresis is given, on the basis of eq 6, by

$$\cos \theta_{\text{adv}} - \cos \theta_{\text{rec}} = \frac{\pi}{4} S_f^2 (\cos \theta_{\text{adv}0} - \cos \theta_{\text{rec}0}) + H_f \quad (10)$$

Figure 7a shows experimental data on the contact angle hysteresis and the theoretical values calculated from eq 10 with  $H_f = c(D/P)^2$ .

$P$ ).<sup>2</sup> Note that the proportionality constant  $c$  is proportional to  $1/D$ . It is observed that the value  $c = 0$  (the only effect of adhesion hysteresis) underestimates the contact angle hysteresis by roughly 50%, meaning that the adhesion hysteresis and roughness contributions are approximately the same order of magnitude, whereas  $c = 0.5$  provides a reasonable fit.

The Cassie–Wenzel transition was observed on evaporating droplets. The droplet radius  $R$  at the Cassie–Wenzel transition was found to be proportional to  $P/D$  (or  $P/H$ ) (Figure 7b), which suggests that the transition is a linear 1D phenomenon and that neither droplet droop (that would involve  $P^2/H$ ) nor droplet weight (that would involve  $R^3$ ) is responsible for the transition but rather linear geometric relations are involved. Note that the experimental values approximately correspond to the values of the ratio  $RD/P = 50 \mu\text{m}$  or the total area of the pillar tops under the droplet  $(\pi D^2/4)\pi R^2/P^2 = 6200 \mu\text{m}^2$ .

Besides the contact angle hysteresis, the asymmetry of the Wenzel and Cassie states is the result of the wetting/dewetting asymmetry. Whereas the fragile metastable Cassie state is often observed as well as its transition to the Wenzel state, the opposite transition never happens. Using eqs 1 and 3, the contact angle with the patterned surfaces is given by

$$\cos \theta = (1 + 2\pi S_f^2) \cos \theta_0 \text{ (Wenzel state)} \quad (11)$$

$$\cos \theta = \frac{\pi}{4} S_f^2 (\cos \theta_0 + 1) - 1 \text{ (Cassie state)} \quad (12)$$

For a perfect macroscale system, the transition between the Wenzel and Cassie states should occur only at the intersection of the two regimes (the point at which the contact angle and net energies of the two regimes are equal, corresponding to  $S_f = 0.51$ ). It is observed, however, that the transition from the metastable Cassie to stable Wenzel state occurs at much lower values of the spacing factor  $0.083 < S_f < 0.111$ .

The static contact angle is shown in Figure 8a as a function of the spacing factor. The solid and dashed straight lines correspond to the theoretical values of the contact angle calculated from eqs 11 and 12 using the value of the contact angle for a nominally flat surface,  $\theta_0 = 109^\circ$ . The two series of experimental data are shown with squares and diamonds. It is observed that the metastable Cassie state can transform into the stable Wenzel state. The intersection of the two theoretical lines corresponding to the two regimes is at the point that corresponds to equal Wenzel and Cassie state free energies, whereas the transition corresponds to a Wenzel state energy that is much lower than the Cassie energy and thus involves significant energy dissipation and is irreversible.

Figure 8b shows the values of the advancing contact angle plotted against the spacing factor. The solid and dashed straight lines correspond to the values of the contact angle for the Wenzel and Cassie states, calculated from eqs 11 and 12 using the advancing contact angle for a nominally flat surface,  $\theta_{\text{adv}0} = 116^\circ$ . It is observed that the calculated values underestimate the advancing contact angle, especially for large  $S_f$  (small distance between the pillars or pitch  $P$ ). This is understandable because the calculation takes into account only the effect of the contact area and ignores the effect of roughness and edge line density (corresponding to  $H_f = 0$  in eq 10), whereas this effect is more pronounced for high pillar density (large  $S_f$ ). In a similar manner, the contact angle is underestimated for the Wenzel state because the pillars constitute a barrier for the advancing droplet.

Figure 8c shows the values of the contact angle after the transition took place (dimmed squares and diamonds), as was observed during evaporation in the ESEM. For both series, the

(43) Jung, Y. C.; Bhushan, B. J. *Microsc.*, in press.

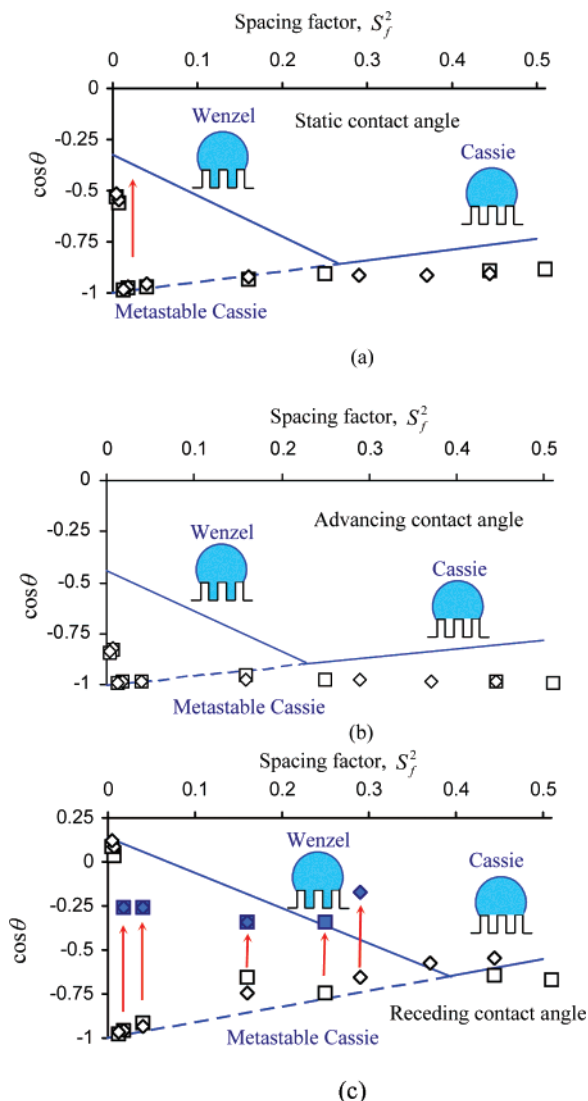


**Figure 8.** Theoretical (—, ---) and experimental ( $\square$  for the first series,  $\diamond$  for the second series). (a) Contact angle as a function of the spacing factor. (b) Advancing contact angle (c) Receding contact angle and values of the contact angle observed after the transition during evaporation (blue).

values almost coincided. For comparison, the values of the receding contact angle measured for millimeter-sized water droplets are also shown (squares and diamonds) because evaporation constitutes removing liquid and thus the contact angle during evaporation should be compared with the receding contact angle. The solid and dashed straight lines correspond to the values of the contact angle, calculated from eqs 14 and 15 using the receding contact angle for a nominally flat surface,  $\theta_{\text{rec0}} = 82^\circ$ . Figure 8c demonstrates good agreement between the experimental data and eqs 11 and 12.

We showed in the present section that an abrupt transition from the metastable Cassie to Wenzel wetting regime is found for micropatterned surfaces. The transition can be observed during microdroplet evaporation in ESEM. The droplet radius at the transition is linearly proportional to the pitch between pillars divided by their diameter. This suggests that interactions at the perimeter of the droplet (rather than in the bulk area beneath the droplet) dominate in the transition. We showed also that the transition cannot be predicted from the macroscale equations for the contact angle and contact angle hysteresis, such as eqs 11 and 12, because it involves micro- and nanoscale interactions. We also found that contact angle hysteresis can be explained to

result from two factors, which act simultaneously. First, the changing contact area affects the hysteresis because a certain value of the contact angle hysteresis is inherent for even a nominally flat surface. Decreasing the contact area by increasing the pitch between the pillars leads to a proportional decrease in the hysteresis. This effect is clearly proportional to the contact area between the solid surface and the liquid droplet. Second, edges of the pillar tops prevent the motion of the triple line. This roughness effect is proportional to the contact line density, and its contribution was, in our experiment, comparable to the contact area effect. Interestingly, the effect of the edges is much more significant for the advancing than for the receding contact angle.

### 5. Conclusions

We investigated the wetting of micropatterned superhydrophobic surfaces by water droplets and found several effects that are specific to the multiscale character of this process. First, we discussed the applicability of the Wenzel and Cassie equations for average surface roughness and heterogeneity. These equations relate the local contact angle with the apparent contact angle of a rough/heterogeneous surface by averaging the former. However, the triple line at which the contact angle is defined has two very different length scales: its width is on the molecular size scale and its length is on the order of the size of the droplet (that is, micrometers or millimeters). Therefore, what should be the size of the roughness/heterogeneity for these equations to be valid? We presented an argument that states that in order for the averaging to be valid, the roughness details should be small compared to the size of the droplet (and not on the order of the molecular size). We showed that whereas for the uniform roughness/heterogeneity the Wenzel and Cassie equations can be applied, for a more complicated case of nonuniform heterogeneity the generalized equations should be used. The proposed generalized Cassie–Wenzel equations are consistent with a broad range of available experimental data. The generalized equations are valid both in the cases when the classical Wenzel and Cassie equations can be applied and in the cases when the latter fail.

The macroscale contact angle hysteresis and Cassie–Wenzel transition cannot be determined from the macroscale equations and are governed by micro- and nanoscale effects, so wetting is a multiscale phenomenon. The kinetic effects associated with the contact angle hysteresis should be studied on the microscale, whereas the effects of the adhesion hysteresis and the Cassie–Wenzel transition involve processes on the nanoscale. Our theoretical arguments are supported by our experimental data on micropatterned surfaces. The experimental study of contact angle hysteresis demonstrates that two different processes are involved: the changing solid–liquid area of contact and pinning of the triple line. The latter effect is more significant for the advancing than for the receding contact angle. The transition between wetting states was observed for evaporating microdroplets in ESEM, and the droplet radius scales well with the geometric parameters of the micropattern. These findings provide new insights into the fundamental mechanisms of wetting and can lead to the creation of successful nonadhesive surfaces.

**Note Added after ASAP Publication.** This article was published ASAP on December 12, 2007. A change has been made in the second paragraph of Section 3. The correct version was published on January 31, 2008.